



A low-background fluorescent aptasensor for acetamiprid detection based on DNA three-way junction-formed G-quadruplexes and graphene oxide

Yunwei Zhao¹ · Hui Zhang¹ · Ying Wang¹ · Yanfang Zhao¹ · Yaowei Li¹ · Lei Han¹ · Lihua Lu¹

Received: 16 November 2020 / Revised: 11 December 2020 / Accepted: 21 December 2020 / Published online: 19 February 2021
© Springer-Verlag GmbH Germany, part of Springer Nature 2021

Abstract

A simple fluorescence detection platform has been established for acetamiprid assay based on DNA three-way junctions (TWJs), which can triple the fluorescence signal without any other amplification. It is designed with three single-stranded DNAs (ssDNA), each of which contains one-third or two-thirds of the G-quadruplex sequence at each end. Upon the addition of acetamiprid, the conformation of the aptamer-containing double-stranded DNA (dsDNA) changes from its original conformation and releases a strand of ssDNA. This ssDNA, with the other two ssDNAs, can assemble into DNA TWJs, and the three pairs of the branched ends of the DNA TWJs are adjacent to each other, allowing them to form three units of G-quadruplexes. Hence, the fluorescence of *N*-methyl mesoporphyrin IX (NMM) is lighted by the nascent G-quadruplexes. Graphene oxide (GO) is then added to minimize the detection background by absorbing the free NMM and non-target-induced ssDNA. The proposed strategy can assay acetamiprid in a wide linear range of 0–500 nM with a detection limit of 5.73 nM. More importantly, this assay platform demonstrates high potential for acetamiprid assay in food control and environmental monitoring.

Keywords DNA three-way junctions · G-quadruplex · Graphene oxide · Nicotinic insecticide · Fluorescent aptasensor

Introduction

With the increasing awareness of the importance of food safety and environmental protection, concerns regarding pesticide residue have become a critical area of focus. Acetamiprid, as one type of nicotinic insecticide, acts on the nicotinic acetylcholine receptor at the synaptic site of the insect nervous system [1]. It has no cross-resistance to organophosphorus, carbamate or pyrethroid insecticides, so it is widely used in pest control [2]. However, the excessive application of pesticides has led to adverse environmental and ecological effects. Research has found that acetamiprid residue in agricultural products can seriously jeopardize human health [3–5]. Therefore, there is an urgent need to explore novel strategies for the efficient and sensitive detection of acetamiprid.

Although traditional chromatographic or antibody-based detection techniques have been used in acetamiprid assay, their shortcomings, including tedious sample preparation procedures, long analysis time and expensive instruments, have hindered their more widespread use [6, 7]. Oligonucleotide-based biosensors have recently been identified as promising alternatives to acetamiprid assay [8–10]. An aptamer is a short strand of oligonucleotide with a certain sequence that can specifically recognize and bind to a target molecule. Because of their easy synthesis, low cost, high stability and strong affinity towards their target under various conditions, aptamers are widely used as recognition units in the fabrication of biosensors [11–14]. Liu and colleagues first discovered the DNA aptamer of acetamiprid (49-nt oligonucleotide sequence S18) [15], which has been commonly used in the specific recognition of acetamiprid. In the presence of acetamiprid, it binds specifically to its aptamer and causes the aptamer to undergo a conformational change. This change can be converted into electrochemical [16–18], colorimetric [19, 20] and luminescence [21, 22] signals, the last of which have attracted the attention of researchers due to their simple operations and rapid signal responses.

✉ Lei Han
hanlei@qau.edu.cn

✉ Lihua Lu
lulihua2012@qau.edu.cn

¹ College of Chemistry and Pharmaceutical Sciences, Qingdao Agricultural University, Qingdao 266109, China

DNA three-way junctions (TWJs) are important building units in the fabrication of DNA supermolecules and dynamic assemblies [23, 24]. They are composed of three double-stranded arms linked at a junction point to form a branched configuration [25], and hence are also referred to as Y-junction DNA. Wang and colleagues [26] developed a target-induced DNA TWJ model which combined electrochemical, fluorescence and colorimetric properties in a supermolecule. Ma and his group built a luminescent cocaine detection platform based on a label-free DNA TWJ molecular switch [25]. The G-quadruplex structure is a DNA secondary motif which has been broadly used in label-free oligonucleotide-based detection. Certain commercially available dyes such as thioflavin T (ThT), crystal violet (CV) and *N*-methyl mesoporphyrin IX (NMM) can specifically recognize the G-quadruplex through the interaction with the G-tetrad plane of the G-quadruplex, and hence emit strong fluorescence. Thus, they are often used as G-quadruplex probes. The combinations of G-quadruplex with these dyes have been widely used as a signal transducer in label-free fluorescence detection.

Graphene oxide (GO) has demonstrated great potential in biosensors. GO can adsorb single-stranded DNA (ssDNA) via the non-covalent π -stacking interaction between its hexagonal rings and ssDNA nucleobases. Conversely, GO cannot adsorb double-stranded DNA (dsDNA) or G-quadruplexes because negatively charged GO are repelled by the phosphate skeletons of dsDNA and G-quadruplexes [27]. For instance, Chu and colleagues [28] developed a G-quadruplex ligand screening platform by virtue of the non-adsorption of GO to G-quadruplex. Due to its unique properties and the fluorescence quenching effect to organic dyes through fluorescence resonance energy transfer (FRET) [29–34], GO can be used to develop a series of simple and universal detection strategies [35].

Inspired by these concepts, a label-free and enzyme-free acetamiprid detection platform was established in this work by using a DNA TWJ-assembled G-quadruplex as a molecular switch and GO as a background reducer. To the best of our knowledge, this is the first report of a pesticides detection platform based on a DNA TWJ-assembled G-quadruplex. The platform demonstrates high potential for use in the facile detection of pesticides in the areas of food control and environmental monitoring.

Methods

Chemicals and materials

Acetamiprid, profenofos, phoxim, chlorpyrifos, metalaxyl, ziram, diethofencarb and atrazine were purchased from Aladdin Chemistry Co. Ltd. (Shanghai, China). *N*-Methyl mesoporphyrin IX (NMM) was purchased from J&K

Scientific Ltd. GO was purchased from Suzhou Carbon Graphene Technology Co. Ltd. Bovine serum albumin (BSA), human serum albumin (HSA), lysozyme and thrombin were purchased from Shanghai Macklin Biochemical Co. Ltd. The involved DNA sequences (Shanghai Sangon Biotech Co. Shanghai, China) are listed in Table 1. The ssDNA was dispersed in Milli-Q water as stock solution (10 μ M), which was stored at -20 °C until use.

Fluorescence assay of acetamiprid

Firstly, AP-1 and SG-1 were heated in Tris-HCl buffer (10 mM Tris, 10 mM MgCl₂, 100 mM NaCl, pH = 7.4) at 95 °C for 5 min and gradually cooled to room temperature within 30 min to promote the hybridization of dsDNA AP-1/SG-1. Subsequently, certain concentrations of acetamiprid and 16 μ L of dsDNA AP-1/SG-1 (5 μ M) were incubated in Tris-HCl buffer (10 mM Tris, 10 mM MgCl₂, 100 mM NaCl, pH=7.4) for 30 min at 25 °C to promote the interaction of acetamiprid and its aptamer [36, 37]. Secondly, 8 μ L of SG-2 (10 μ M) and 8 μ L of SG-3 (10 μ M) were added to the reaction solution to facilitate the assembly of the released SG-1 with SG-2 and SG-3 into DNA TWJs. At the same time, 10 μ L of 2 M KCl was added to the solution to promote the formation of G-quadruplexes. After 60 min incubation, 5 μ L of NMM (100 μ M) was dropped into the system and the solution was thoroughly mixed for its specific binding to the nascent G-quadruplexes. Finally, 12 μ L of GO (50 μ g·mL⁻¹) was added to the system. A certain volume of Tris-HCl buffer (10 mM, pH = 7.4) was added to reach a final detection volume of 200 μ L. The fluorescence intensity measured in the test group (with acetamiprid) was reported as *F*, and the fluorescence intensity measured in the control group (without acetamiprid) was reported as *F*₀. Then, each factor was estimated using the relative intensity *F* – *F*₀. The fluorescence spectra were recorded on a fluorescence spectrometer (F-7000, Hitachi, Japan), which were measured under the excitation of λ_{ex} = 399 nm.

Table 1 The DNA sequences employed in this project^a

DNA	Sequences (from 5' to 3')
AP-1	CTGACACCATATTATGAAGA
SG-1	GTG₃TAG₃CGCATAATATGGTGG₂T₂G₂
SG-2	GTG₃TAG₃CGCACC ATCAATATGCG ₃ ATG ₃ TG
SG-3	G₂T₂G₂ATATTGATTATGG₂T₂G₂

^a The underlined and italic bases are initially complementary to each other. The bold bases are G-rich DNA sequences

Detection of acetaminophen in food or lake water samples

For the acetaminophen analysis in apple extract or lake water, 16 μL of AP-1/SG-1 (5 μM) and 2 μL of concentrated apple samples or 20 μL of filtered lake water samples were added to Tris-HCl buffer (10 mM, pH = 7.4). Then, various amounts of acetaminophen (final concentrations of 50, 200, 500 nM, respectively) were dropped into the mixtures of diluted apple extract or lake water samples. The next experimental steps are the same those as outlined above.

Results and discussion

The principle of acetaminophen assay

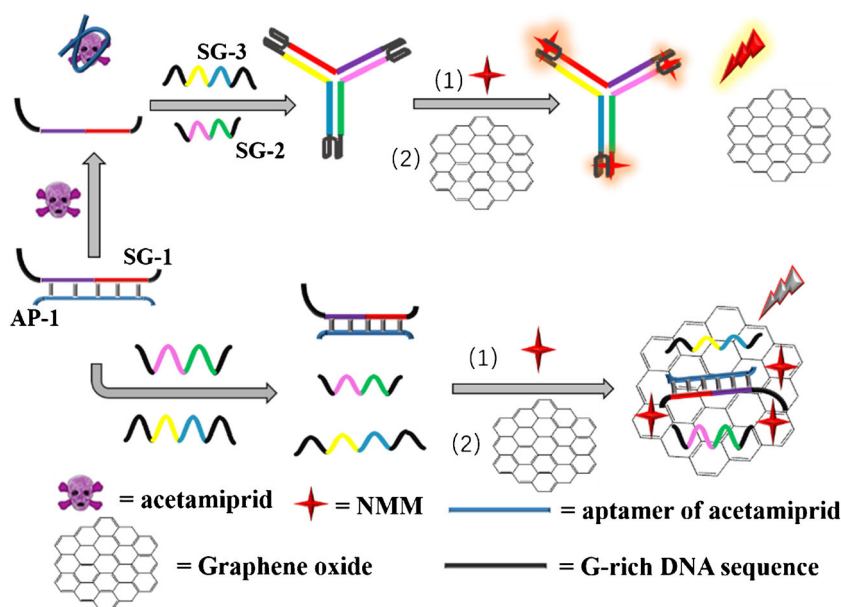
The detection mechanism for acetaminophen assay is schematically illustrated in Scheme 1. Four ssDNAs, i.e., AP-1, SG-1, SG-2 and SG-3, are involved in this detection. AP-1 is the aptamer DNA, and SG-1, SG-2 and SG-3 hang one-third or two-thirds of G-quadruplex DNA sequences at both ends. Initially, AP-1 and SG-1 form the duplex DNA AP-1/SG-1 through their partial complementary sequences (12 bases). In the presence of acetaminophen, AP-1 preferentially combines with acetaminophen, and SG-1 is released from AP-1/SG-1. Then, the addition of SG-2 and SG-3 induces the formation of DNA TWJs through their interactive complementary DNA sequences. With the aid of K^+ , the ends of the three-way branches (black part) form three units of G-quadruplexes. The added NMM can be inserted into the G-quadruplexes and produce intense fluorescence. This fluorescence cannot be quenched by the subsequent addition of GO because of

the protection by the nascent G-quadruplexes. Without acetaminophen, SG-1 cannot be released from dsDNA AP-1/SG-1. Thus, the subsequent addition of SG-2 and SG-3 cannot lead to the formation of DNA TWJs. Accordingly, no G-quadruplex forms, and the added NMM cannot induce strong fluorescence. This is because the GO quenches the fluorescence in the detection system via simultaneous adsorption of SG-2, SG-3, ssDNA-hung AP-1/SG-1 and free NMM.

The feasibility of acetaminophen detection based on DNA TWJs and GO

To verify the feasibility of the proposed detection method, its fluorescence responses under different conditions were investigated. In the absence of acetaminophen, the solution system contains AP-1/SG-1, SG-2, SG-3, NMM and GO and just shows minimal fluorescence (Fig. 1A, curve a). Upon the addition of acetaminophen, the system exhibits highly enhanced fluorescence (Fig. 1A, curve b). These results indicate that the DNA TWJ-assembled G-quadruplexes form in the presence of acetaminophen, confirming the detection ability of the developed strategy. Comparing the fluorescence intensities between the GO-added system (Fig. 1A, curve a) with the GO-free system (Fig. 1A, c), it is found that the fluorescence intensity of the GO-added system is significantly weaker than that of the GO-free system, confirming the obvious background signal inhibition by GO. The detection still works in the absence of GO (Supplementary Information [ESM], Scheme S1), but presents a much smaller signal change (ESM, Fig. S1) after the addition of acetaminophen, which adversely affects the detection sensitivity. In addition, the zeta potential was tested to monitor the detection process. The zeta potential of GO is -7.54 mV (ESM, Fig. S2, a), which is

Scheme 1 Schematic illustration of the acetaminophen detection based on DNA TWJs and GO. In step (1), after the addition of NMM, it can be inserted into the G-quadruplexes and produce intense fluorescence. In step (2), upon the addition of GO, it cannot quench the fluorescence of NMM because of the protection from the combination of G-quadruplexes/NMM



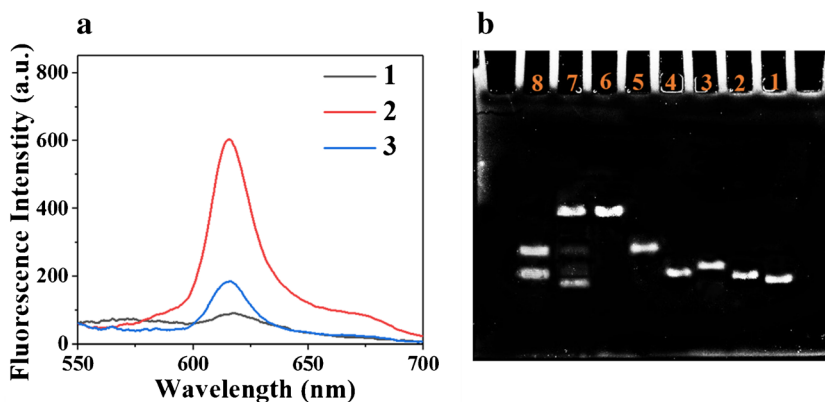


Fig. 1 (A) Fluorescence responses of the detection system towards various conditions. (a) AP-1/SG-1 + SG-2 + SG-3 + NMM + GO, (b) AP-1/SG-1 + acetamidiprid + SG-2 + SG-3 + NMM + GO, (c) AP-1/SG-1 + SG-2 + SG-3 + NMM. The concentrations of acetamidiprid, AP-1/SG-1, SG-2, SG-3, NMM and GO were 500 nM, 400 nM, 400 nM, 400 nM, 2.5 μM and 3 $\mu\text{g}\cdot\text{mL}^{-1}$, respectively. (B) PAGE analysis. Track 1, AP-1;

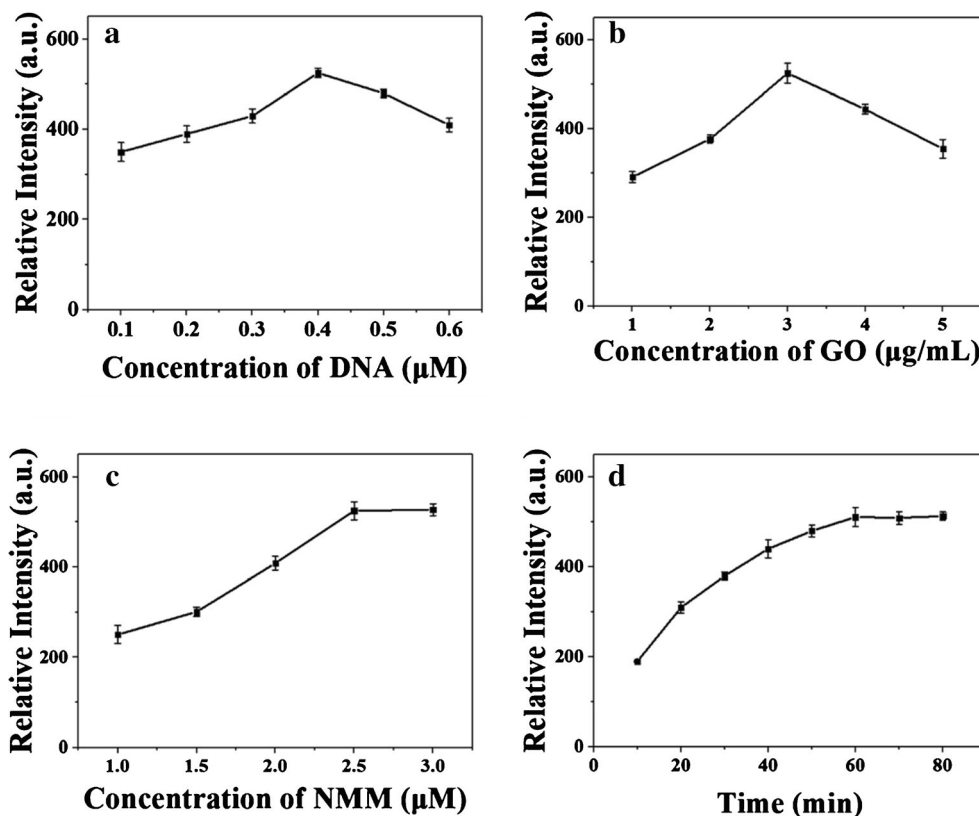
track 2, SG-3; track 3, SG-2; track 4, SG-1; track 5, AP-1/SG-1; track 6, DNA TWJs formed by SG-1, SG-2 and SG-3; track 7, AP-1/SG-1+ acetamidiprid + SG-2 + SG-3; track 8, AP-1/SG-1 + SG-2 + SG-3. The concentrations of AP-1/SG-1, SG-2, SG-3 and acetamidiprid were 400 nM, 400 nM, 400 nM and 500 nM, respectively

mainly caused by the ionization of the $-\text{COOH}$ and $-\text{OH}$ groups on its surface [38]. In the presence of DNA solution, the negatively charged ssDNA SG-2 and SG-3 interact with GO through hydrophobic $\pi-\pi$ stacking effects [39], resulting in more negative zeta potential of GO than that of GO only (ESM, Fig. S2, b). Upon the addition of acetamidiprid, the DNA three-way junction G-quadruplexes form in the detection system. Due to the strong interaction with the G-quadruplexes,

K^+ on the GO surface moves away from the surface, and this leads to more negative zeta potential (ESM, Fig. S2, c).

To further confirm the detection ability, polyacrylamide gel electrophoresis (PAGE) was performed. As shown in Fig. 1B, AP-1, SG-3, SG-2, SG-1, AP-1/SG-1 and DNA TWJs show clear bands in track 1, track 2, track 3, track 4, track 5 and track 6, respectively. Track 1, track 2, track 3 and track 4 are loaded with ssDNA, which run faster than track 5 since track 5

Fig. 2 Relative fluorescence intensities of the detection system versus (a) the concentrations of DNA (0.1, 0.2, 0.3, 0.4, 0.5 and 0.6 μM) (the system contained 500 nM of acetamidiprid, 3 $\mu\text{g}\cdot\text{mL}^{-1}$ of GO, 2.5 μM of NMM and 100 mM of K^+), (b) the concentrations of GO (1, 2, 3, 4 and 5 $\mu\text{g}\cdot\text{mL}^{-1}$) (the system contained 500 nM of acetamidiprid, 0.4 μM of DNA, 2.5 μM of NMM and 100 mM of K^+), (c) the concentrations of NMM (1.0, 1.5, 2.0, 2.5 and 3.0 μM) (the system contained 500 nM of acetamidiprid, 0.4 μM of DNA, 3 $\mu\text{g}\cdot\text{mL}^{-1}$ of GO and 100 mM of K^+), and (d) incubation time (10, 20, 30, 40, 50, 60, 70 and 80 min, respectively) (the system contained 500 nM of acetamidiprid, 0.4 μM of DNA, 3 $\mu\text{g}\cdot\text{mL}^{-1}$ of GO, 2.5 μM of NMM and 100 mM of K^+)



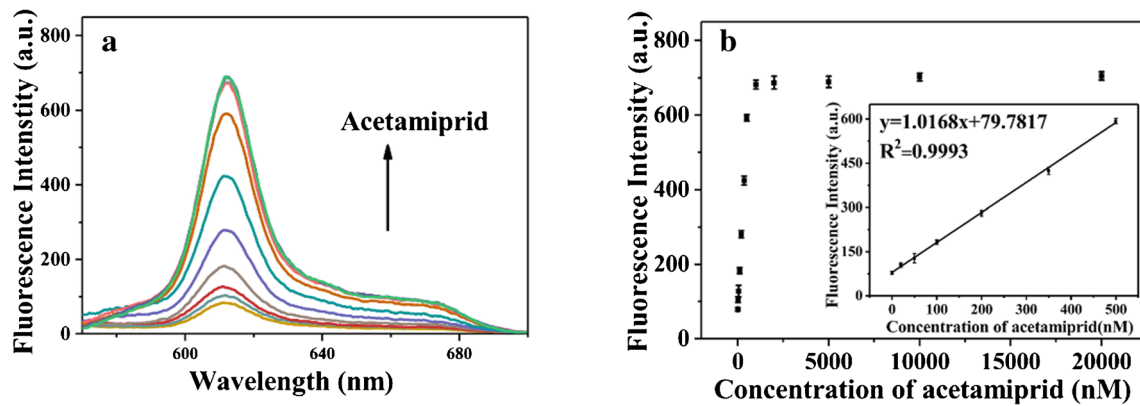


Fig. 3 (a) The fluorescence responses of NMM towards different concentrations (0, 20, 50, 100, 200, 350, 500, 1000, 2000, 5000, 10,000 and 20,000 nM) of acetamiprid. (b) The fluorescence intensities

of NMM in response to different concentrations of acetamiprid. The concentrations of NMM, DNA and GO were 2.5 μM , 0.4 μM and 3 $\mu\text{g}\cdot\text{mL}^{-1}$, respectively

Table 2 Comparison of analytical performance for different acetamiprid assays

Methods	Detection limit (LOD)	Linear range	Reference
A low-background fluorescent aptasensor for acetamiprid detection based on DNA three-way junction-jointly formed G-quadruplexes	5.73 nM	20–500 nM	This work
A nitrile-mediated aptasensor for optical anti-interference detection of acetamiprid in apple juice by surface-enhanced Raman scattering	6.8 nM	25–250 nM	[41]
Fabrication of a novel label-free aptasensor for acetamiprid by fluorescence resonance energy transfer between $\text{NH}_2\text{-NaYF}_4\text{: Yb, Ho@SiO}_2$ and Au nanoparticles	3.2 nM	50–1000 nM	[3]
A highly selective electrochemical impedance spectroscopy-based aptasensor for sensitive detection of acetamiprid	1 nM	5–600 nM	[42]
A facile label-free colorimetric aptasensor for acetamiprid based on the peroxidase-like activity of hemin-functionalized reduced graphene oxide	40 nM	100–10,000 nM	[43]
Fluorometric aptasensing of the neonicotinoid insecticide acetamiprid using multiple complementary strands and gold nanoparticles	2.8 nM	5–50 nM	[44]
Acetamiprid multi-detection by disposable electrochemical DNA aptasensor	86 nM	0.25–2.0 μM	[18]
Aptamer-containing triple-helix molecular switch for rapid fluorescence sensing of acetamiprid	9.12 nM	100–1200 nM	[45]
Aptamer-based colorimetric sensing of acetamiprid in soil samples: sensitivity, selectivity and mechanism	5 nM	75 nM–7.5 μM	[19]
Aptamer-based fluorescence screening assay for acetamiprid via inner filter effect of gold nanoparticles on the fluorescence of CdTe quantum dots	7.29 nM	0.05–1 μM	[46]
Application of solid-phase extraction and liquid chromatography-mass spectrometry to the determination of neonicotinoid pesticide residues in fruits and vegetables	90 nM	0.22–2.2 μM	[47]
Analysis of nicotinoid insecticide residues in honey by solid matrix partition clean-up and liquid chromatography-electrospray mass spectrometry	135 nM	2.25–22.5 μM	[48]
A colorimetric detection method for pesticide acetamiprid by fine-tuning aptamer length	400 nM		[49]
In-coupled syringe-assisted octanol-water partition microextraction coupled with high-performance liquid chromatography for simultaneous determination of neonicotinoid insecticide residues in honey	0.25 $\text{ng}\cdot\text{mL}^{-1}$ (1.12 nM)	0.1–3000 $\text{ng}\cdot\text{mL}^{-1}$	[50]
Reduction of hazardous organic solvent in sample preparation for hydrophilic pesticide residues in agricultural products with conventional liquid chromatography	5 $\text{ng}\cdot\text{mL}^{-1}$ (22 nM)	0.005–2 $\mu\text{g}\cdot\text{mL}^{-1}$	[51]
Determination of neonicotinoid pesticide residues in agricultural samples by solid-phase extraction combined with liquid chromatography–tandem mass spectrometry	0.01 $\text{mg}\cdot\text{kg}^{-1}$ (44.9 nM)	0.05–3.6 $\text{mg}\cdot\text{kg}^{-1}$	[6]
Health risk assessment of neonicotinoid insecticide residues in pistachio using a QuEChERS-based method in combination with high-performance liquid chromatography-ultraviolet detection	20 $\mu\text{g}\cdot\text{L}^{-1}$ (89.8 nM)	20–2500 $\mu\text{g}\cdot\text{L}^{-1}$	[52]
Development of an upconversion fluorescence DNA probe for the detection of acetamiprid by magnetic nanoparticle separation	0.65 $\mu\text{g}\cdot\text{L}^{-1}$ (2.9 nM)	0.89–14.18 $\mu\text{g}\cdot\text{L}^{-1}$	[53]
A novel optical sensor based on carbon dot-embedded molecularly imprinted silica for selective acetamiprid detection	2 nM	7–107 nM	[54]
Immunoassay for acetamiprid detection: application to residue analysis and comparison with liquid chromatography	0.053 $\text{ng}\cdot\text{g}^{-1}$ (23.8 pM)	0.18–3 $\text{ng}\cdot\text{g}^{-1}$	[55]

loaded the duplex DNA AP-1/SG-1. As expected, track 6 is the slowest runner among all tracks since it is loaded with the assembled DNA TWJs by SG-1, SG-2 and SG-3. The mixture containing AP-1/SG-1, acetamiprid, SG-2 and SG-3 is loaded in track 7. It is found that in track 7, a band appears with the same site as that in track 6, indicating that the DNA TWJs are generated upon the addition of acetamiprid. Without acetamiprid, in track 8 there is no band corresponding to the DNA TWJs in track 6, showing no formation of DNA TWJs in the absence of acetamiprid. The PAGE results firmly validate the feasibility of the DNA TWJs designed using this strategy.

Optimization of the DNA TWJs and GO-based fluorescence acetamiprid assay

The experimental conditions involved in this assay are then optimized, including the concentrations of DNA, GO and NMM, the formation time of the DNA TWJs and the concentration of K^+ . One molecule of acetamiprid binds to one strand of AP-1, and one molecule of DNA TWJs needs one molecule of SG-1, SG-2 and SG-3, respectively. Thus, the molar ratio of AP-1/SG-1, SG-2 and SG-3 is fixed at 1:1:1 in the optimization of the DNA concentration. Figure 2a shows that the relative fluorescence intensity rapidly increases with increasing DNA concentration. When the DNA concentration reaches 0.4 μM , the relative fluorescence intensity begins to decrease, which is because the additional DNA influences the adsorption of GO towards ssDNA, and the background signal increases in the detection. As shown in Fig. 2b, 3 $\mu\text{g}\cdot\text{mL}^{-1}$ of GO produces the highest relative fluorescence intensity. This may be because the low concentration of GO cannot completely quench the fluorescence of NMM, while the high concentration of GO may quench the fluorescence of the G-quadruplex-protected NMM. The assembly of DNA TWJs is very important in this detection, so the incubation time of DNA TWJs is also investigated. As shown in Fig. 2c, the result indicates that the highest fluorescence intensity is observed at 2.5 μM of NMM, which is ascribed to the weak signal or high background of the system at lower or higher concentrations of NMM, respectively. As shown in Fig. 2d, the relative fluorescence intensity increases when the incubation time is increased from 5 min to 60 min, but no significant increase is produced with a further increase in incubation time. The concentration of K^+ is also studied because of its important role in the stabilization of the G-quadruplex structure. As shown in Fig. S4, the optimal concentration of K^+ is 100 mM.

Analytical performance of the acetamiprid assay based on DNA TWJs and GO

In order to examine the performance of the acetamiprid detection platform, the fluorescence intensity of the detection system is investigated by titration experiments using various concentrations of acetamiprid under the optimized conditions. In Fig. 3a, as the

concentration of acetamiprid increases, the fluorescence intensity increases gradually in the range of 0–500 nM. This indicates that an increasing number of DNA TWJs are formed with the increase in acetamiprid concentration and result in enhanced emission intensity. When the concentration of acetamiprid is increased beyond 500 nM, the fluorescence intensity of the system shows a minimal further increase in fluorescence. Based on the fluorescence intensity increase, the concentration level of acetamiprid can be estimated. Figure 3b shows that the fluorescence intensity has a good linear relationship with the acetamiprid concentrations in the range of 0–500 nM, which is described in the equation $y = 1.0168x + 79.7817$ ($R^2 = 0.9993$). Based on the linear relationship, the limit of detection (LOD) for the acetamiprid assay was estimated to be 5.73 nM ($3\sigma/\text{slope}$), which is comparable or superior to those reported in Table 2. More importantly, the LOD of acetamiprid is much lower than the legal acetamiprid limit of 0.8 ppm (about 3.59 μM) in foodstuffs [40].

Selectivity of acetamiprid assay based on DNA TWJs and GO

The specificity of this assay is verified by studying its fluorescence responses to other pesticides. The structures of acetamiprid and other pesticides are listed in ESM Fig. S3. The concentration of acetamiprid was 500 nM, and the other pesticides were used at a concentration of 2.5 μM . As shown in Fig. 4, compared with acetamiprid, the relative fluorescence intensities of profenofos, phoxim, chlorpyrifos, metalaxyl, ziram, diethofencarb, atrazine, imidacloprid isocarbophos and clothianidin show only minimal fluorescence changes. In order to further confirm the anti-interference ability of this

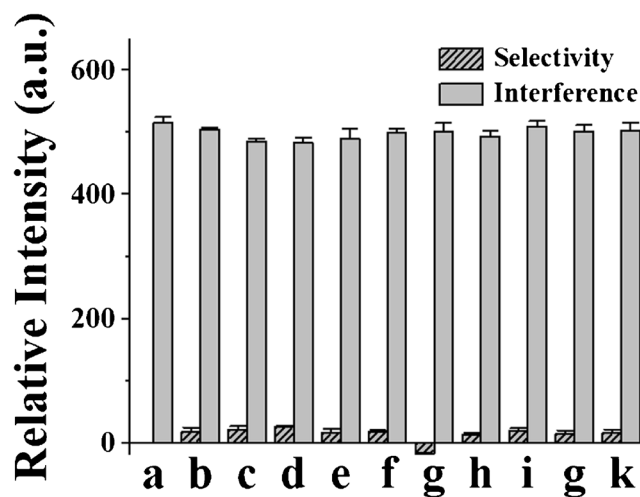


Fig. 4 The relative enhanced fluorescence response to different pesticides (a) acetamiprid, (b) profenofos, (c) phoxim, (d) chlorpyrifos, (e) metalaxyl, (f) ziram, (g) diethofencarb, (h) atrazine, (i) imidacloprid, (g) isocarbophos and (k) clothianidin. The concentration of acetamiprid was 500 nM, and the other pesticides were used at a concentration of 2.5 μM . The error bars represent the standard deviation of three repeated measurements

Table 3 Determination of acetamiprid spiked in diluted lake water or apple extract

Sample No.	Added acetamiprid (nM)	Detected acetamiprid (nM)	SD (<i>n</i> = 5)	Recovery (%)
lake water 1	50	47.7	2.1	95.4
lake water 2	200	211.4	4.3	105.7
lake water 3	500	482.5	5.1	96.5
Apple 1	50	48.0	2.4	96.0
Apple 2	200	207.2	1.9	103.6
Apple 3	500	497.7	5.9	99.5

detection platform, various proteins (BSA, HSA, lysozyme and thrombin) were also tested. ESM Fig. S5 shows that no obvious fluorescence change appears in the presence of five-fold excess proteins. The fluorescence of the mixtures of acetamiprid and other pesticides is also studied. It is observed that the addition of other pesticides in the acetamiprid detection system has little adverse effect on the fluorescence intensity of the solution. Obviously, the experimental results demonstrate good selectivity and anti-interference ability due to the specific combination of acetamiprid with its aptamer. In order to further confirm the selectivity and anti-interference ability of this detection platform, common proteins including bovine serum albumin (BSA), human serum albumin (HSA), lysozyme and thrombin were also tested. ESM Fig. S5 shows that no obvious fluorescence change appears in the presence of fivefold excess proteins.

Repeatability and stability of acetamiprid assay based on DNA TWJs and GO

The repeatability and stability of the detection platform are then studied. As shown in ESM Fig. S6, under the same detection conditions, the fluorescence intensities of seven samples are measured. The results show good reproducibility. The stability of the detection system is investigated by monitoring the fluorescence intensity of the detection platform. ESM Fig. S7 shows that the fluorescence intensity of the detection system is unvaried over a period of 2 h, which indicates that the stability of the fluorescence is long enough for detection.

Real sample detection

As a highly effective insecticide, acetamiprid is widely used for pesticide control in fruits and vegetables. In order to demonstrate its application in food safety and environmental monitoring fields, the detection platform is also used to assay acetamiprid in lake water and apple extract, respectively. Three different concentrations (50, 200, 500 nM) of acetamiprid are added to tenfold diluted lake water or 100-fold diluted apple extract for five repeated measurements.

Recovery values from 95.4% to 105.7% are obtained in the lake water and apple extract samples (Table 3). As shown in ESM, Fig. S8, the fluorescent aptasensor exhibits the similar results as those of high-performance liquid chromatography results for lake water or apple extract samples, verifying its robustness in real sample detection. This shows that the strategy for the determination of acetamiprid is reliable and accurate in real samples.

Conclusion

In this work, a label-free and enzyme-free detection platform based on DNA TWJs and GO has been successfully developed to detect acetamiprid. The developed acetamiprid detection platform can triple the fluorescence signal through DNA TWJ G-quadruplexes. The detection platform has a low background due to the fluorescence quenching of GO towards NMM and ssDNA. The detection of acetamiprid shows high selectivity and anti-interference ability, with a detection limit of 5.73 nM. The assay system contains only one strand of dsDNA, two strands of ssDNA and non-modified GO, which is enzyme-free and label-free. More importantly, the developed strategy exhibits high application potential in food control and environmental monitoring fields.

Supplementary Information The online version contains supplementary material available at <https://doi.org/10.1007/s00216-020-03141-2>.

Acknowledgments This work was funded by the National Natural Science Foundation of China (No. 21705089 and 21705087), the Project of Shandong Province Higher Educational Science and Technology Program (J17KA109 and J18KA067), the Science and Technology Program of Qingdao (No.18-6-1-83-nsh) and the Research Foundation for Distinguished Scholars of Qingdao Agricultural University (663-1117015).

Compliance with ethical standards

Conflict of interest The authors declare that there are no conflicts of interest.

References

- Madianos L, Tsekenis G, Skotadis E, Patsiouras L, Tsoukalas D. A highly sensitive impedimetric aptasensor for the selective detection of acetamiprid and atrazine based on microwires formed by platinum nanoparticles. *Biosens Bioelectron.* 2017;101:268–74.
- Szendrei Z, Edward G, Adam B, Amos Z. Resistance to neonicotinoid insecticides in field populations of the Colorado potato beetle (Coleoptera: Chrysomelidae). *Pest Manag Sci.* 2012;68:941–6.
- Hu W, Chen Q, Li H, Ouyang Q, Zhao J. Fabricating a novel label-free aptasensor for acetamiprid by fluorescence resonance energy transfer between $\text{NH}_2\text{-NaYF}_4\text{:Yb, Ho@SiO}_2$ and au nanoparticles. *Biosens Bioelectron.* 2016;80:398–404.
- Liu X, Su L, Zhu L, Gao X, Wang Y, Bai F, et al. Hybrid material for enrofloxacin sensing based on aptamer-functionalized magnetic nanoparticle conjugated with upconversion nanoprobe. *Sens Actuators B: Chem.* 2016;233:394–401.
- Kaur RP, Gupta V, Christopher AF, Bansal P. Potential pathways of pesticide action on erectile function – a contributory factor in male infertility. *Asian Pac J Reprod.* 2015;4:322–30.
- Xie W, Han C, Qian Y, Ding H, Chen X, Xi J. Determination of neonicotinoid pesticides residues in agricultural samples by solid-phase extraction combined with liquid chromatography–tandem mass spectrometry. *J Chromatogr A.* 2011;1218:4426–33.
- Watanabe E, Yamasaki T, Hirakawa Y, Harada A, Iwasa S, Miyake S. Organic solvent-free immunoassay for quantitative detection of neonicotinoid acetamiprid residues in agricultural products. *Anal Methods.* 2018;10:3162–9.
- Hassani S, Momtaz S, Vakhshiteh F, Maghsoudi AS, Ganjali MR, Norouzi P, et al. Biosensors and their applications in detection of organophosphorus pesticides in the environment. *Arch Toxicol.* 2017;91:109–30.
- Fei A, Liu Q, Huan J, Qian J, Dong X, Qiu B, et al. Label-free impedimetric aptasensor for detection of femtomole level acetamiprid using gold nanoparticles decorated multiwalled carbon nanotube-reduced graphene oxide nanoribbon composites. *Biosens Bioelectron.* 2015;70:122–9.
- Verdian A. Apta-nanosensors for detection and quantitative determination of acetamiprid – a pesticide residue in food and environment. *Talanta.* 2018;176:456–64.
- Dhiman A, Kalra P, Bansal V, Bruno JG, Sharma TK. Aptamer-based point-of-care diagnostic platforms. *Sens Actuators B: Chem.* 2017;246:535–53.
- Selvolini G, Băjan I, Hosu O, Cristea C, Săndulescu R, Marrazza G. DNA-based sensor for the detection of an organophosphorus pesticide: Profenofos. *Sensors.* 2018;18:2035.
- Kim Y, Raston NH, Gu M. Aptamer-based nanobiosensors. *Biosens Bioelectron.* 2016;76:2–19.
- Liu S, Chen Q, Wang Z, Cao T, Zhao G, Zhou Y. Monitoring 2,3',5,5'-tetrachlorobiphenyl with a rapid and sensitive environmental aptamer sensor. *Analyst.* 2019;144:4841–7.
- He J, Liu Y, Fan M, Liu X. Isolation and identification of the DNA aptamer target to Acetamiprid. *J Agric Food Chem.* 2011;59:1582–6.
- Sobhani R, Rezaei B, Shahshahanipour M, Ensafi AA, Mohammadnezhad G. Simple and green synthesis of carbon dots (CDs) from valerian root and application of modified mesoporous boehmite (AlOOH) with CDs as a fluorescence probe for determination of imipramine. *Anal Bioanal Chem.* 2019;411:3115–24.
- Nasr-Esfahani P, Ensafi AA, Rezaei B. Fabrication of a highly sensitive and selective modified electrode for imidacloprid determination based on designed nanocomposite graphene quantum dots/ionic liquid/multiwall carbon nanotubes/polyaniline. *Sens Actuators B: Chem.* 2019;296:126682.
- Rapini R, Cincinelli A, Marrazza G. Acetamiprid multidetection by disposable electrochemical DNA aptasensor. *Talanta.* 2016;161:15–21.
- Shi H, Zhao G, Liu M, Fan L, Cao T. Aptamer-based colorimetric sensing of acetamiprid in soil samples: sensitivity, selectivity and mechanism. *J Hazard Mater.* 2013;260:754–61.
- Yang W, Wu Y, Tao H, Zhao J, Chen H, Qiu S. Ultrasensitive and selective colorimetric detection of acetamiprid pesticide based on the enhanced peroxidase-like activity of gold nanoparticles. *Anal Methods.* 2017;9:5484–93.
- Lin B, Yu Y, Li R, Cao Y, Guo M. Turn-on sensor for quantification and imaging of acetamiprid residues based on quantum dots functionalized with aptamer. *Sens Actuators B: Chem.* 2016;229:100–9.
- Wang J, Wu Y, Zhou P, Yang W, Tao H, Qiu S, et al. A novel fluorescent aptasensor for ultrasensitive and selective detection of acetamiprid pesticide based on the inner filter effect between gold nanoparticles and carbon dots. *Analyst.* 2018;143:5151–60.
- Chen J, Zhou S. Label-free DNA Y junction for bisphenol A monitoring using exonuclease III-based signal protection strategy. *Biosens Bioelectron.* 2016;77:277–83.
- Du Y, Peng P, Li T. Logic circuit controlled multi-responsive branched DNA scaffolds. *Chem Commun.* 2018;54:6132–5.
- Ma D-L, Wang M, He B, Yang C, Wang W, Leung C-H. A luminescent cocaine detection platform using a Split G-quadruplex-selective iridium(III) complex and a three-way DNA junction architecture. *ACS Appl Mater Interfaces.* 2015;7:19060–7.
- Zhang L, Guo S, Zhu J, Zhou Z, Li T, Li J, et al. Engineering DNA three-way junction with multifunctional moieties: sensing platform for bioanalysis. *Anal Chem.* 2015;87:11295–300.
- Li X, Wang G, Ding X, Chen Y, Gou Y, Lu Y. A “turn-on” fluorescent sensor for detection of Pb^{2+} based on graphene oxide and G-quadruplex DNA. *Phys Chem Chem Phys.* 2013;15:12800–4.
- Wang H, Chen T, Wu S, Chu X, Yu R. A novel biosensing strategy for screening G-quadruplex ligands based on graphene oxide sheets. *Biosens Bioelectron.* 2012;34:88–93.
- He S, Song B, Li D, Zhu C, Qi W, Wen Y, et al. A graphene Nanoprobe for rapid, sensitive, and multicolor fluorescent DNA analysis. *Adv Funct Mater.* 2010;20:453–9.
- Xing X-J, Liu X-G, Yue H, Luo Q-Y, Tang H-W, Pang D-W. Graphene oxide based fluorescent aptasensor for adenosine deaminase detection using adenosine as the substrate. *Biosens Bioelectron.* 2012;37:61–7.
- Bi S, Zhao T, Luo B. A graphene oxide platform for the assay of biomolecules based on chemiluminescence resonance energy transfer. *Chem Commun.* 2012;48:106–8.
- Li J, Lu C-H, Yao Q-H, Zhang X-L, Liu J-J, Yang H-H, et al. A graphene oxide platform for energy transfer-based detection of protease activity. *Biosens Bioelectron.* 2011;26:3894–9.
- Gao L, Lian C, Zhou Y, Yan L, Li Q, Zhang C, et al. Graphene oxide–DNA based sensors. *Biosens Bioelectron.* 2014;60:22–9.
- Zhu D, Wang L, Xu X, Jiang W. Label-free and enzyme-free detection of transcription factors with graphene oxide fluorescence switch-based multifunctional G-quadruplex-hairpin probe. *Biosens Bioelectron.* 2016;75:155–60.
- Park J-W, Tatavarty R, Kim DW, Jung H-T, Gu MB. Immobilization-free screening of aptamers assisted by graphene oxide. *Chem Commun.* 2012;48:2071–3.
- Yan Y, Li H, Liu Q, Hao N, Mao H, Wang K. A facile strategy to construct pure thiophene-sulfur-doped graphene/ZnO nanoplates sensitized structure for fabricating a novel “on-off-on” switch photoelectrochemical aptasensor. *Sens Actuators B: Chem.* 2017;251:99–107.
- Xu Y, Zhang W, Shi J, Li Z, Huang X, Zou X, et al. Impedimetric aptasensor based on highly porous gold for sensitive detection of

- acetamiprid in fruits and vegetables. *Food Chem.* 2020;322:126762.
38. Zhu C, Zhai J, Wen D, Dong S. Graphene oxide/polypyrrole nanocomposites: one-step electrochemical doping, coating and synergistic effect for energy storage. *J Mater Chem.* 2012;22:6300–6.
 39. Jang H, Kim YK, Kwon HM, Yeo WS, Min DH. A graphene-based platform for the assay of duplex-DNA unwinding by helicase. *Angew Chem.* 2010;49:5703–7.
 40. Handford CE, Elliott CT, Campbell K. A review of the global pesticide legislation and the scale of challenge in reaching the global harmonization of food safety standards. *Integr Environ Assess Manage.* 2015;11:525–36.
 41. Sun Y, Li Z, Huang X, Zhang D, Zou X, Shi J, et al. A nitrile-mediated aptasensor for optical anti-interference detection of acetamiprid in apple juice by surface-enhanced Raman scattering. *Biosens Bioelectron.* 2019;145:111672.
 42. Fan L, Zhao G, Shi H, Liu M, Li Z. A highly selective electrochemical impedance spectroscopy-based aptasensor for sensitive detection of acetamiprid. *Biosens Bioelectron.* 2013;43:12–8.
 43. Yang Z, Qian J, Yang X, Jiang D, Du X, Wang K, et al. A facile label-free colorimetric aptasensor for acetamiprid based on the peroxidase-like activity of hemin-functionalized reduced graphene oxide. *Biosens Bioelectron.* 2015;65:39–46.
 44. Bahreyni A, Yazdian-Robati R, Ramezani M, Abnous K, Taghdisi SM. Fluorometric aptasensing of the neonicotinoid insecticide acetamiprid by using multiple complementary strands and gold nanoparticles. *Microchim Acta.* 2018;185:272–9.
 45. Liu X, Li Y, Liang J, Zhu W, Xu J, Su R, et al. Aptamer contained triple-helix molecular switch for rapid fluorescent sensing of acetamiprid. *Talanta.* 2016;160:99–105.
 46. Guo JJ, Li Y, Wang LK, Xu JY, Huang YJ, Luo YL, et al. Aptamer-based fluorescent screening assay for acetamiprid via inner filter effect of gold nanoparticles on the fluorescence of CdTe quantum dots. *Anal Bioanal Chem.* 2016;408:557–66.
 47. Muccio AD, Paola F, Danilo Attard B, Roberto D, Serenella S, Patrizia M. Application of solid-phase extraction and liquid chromatography–mass spectrometry to the determination of neonicotinoid pesticide residues in fruit and vegetables. *J Chromatogr A.* 2006;1108:1–6.
 48. Fidente P, Serenella S, Fabiana V, Patrizia M. Analysis of nicotinoid insecticides residues in honey by solid matrix partition clean-up and liquid chromatography–electrospray mass spectrometry. *J Chromatogr A.* 2005;1094:175–8.
 49. Tian Y, Wang Y, Sheng Z, Li T, Li X. A colorimetric detection method of pesticide acetamiprid by fine-tuning aptamer length. *Anal Biochem.* 2016;513:87–92.
 50. Vichapong J, Burakham R, Srijarana S. In-coupled syringe assisted octanol-water partition microextraction coupled with high-performance liquid chromatography for simultaneous determination of neonicotinoid insecticide residues in honey. *Talanta.* 2015;139:21–6.
 51. Watanabe E, Kobara Y, Baba K, Eun H. Reduction of hazardous organic solvent in sample preparation for hydrophilic pesticide residues in agricultural products with conventional liquid chromatography. *J Agric Food Chem.* 2013;61:4792–8.
 52. Mahdavi V, Garshasbi Z, Farimani MM, Farhadpour M, Aboul-Enein HY. Health risk assessment of neonicotinoid insecticide residues in pistachio using a QuEChERS-based method in combination with HPLC-UV. *Biomed Chromatogr.* 2020;34:e4747.
 53. Sun N, Ding Y, Tao Z, You H, Hua X, Wang M. Development of an upconversion fluorescence DNA probe for the detection of acetamiprid by magnetic nanoparticles separation. *Food Chem.* 2018;257:289–94.
 54. Poshteh Shirani M, Rezaei B, Ensafi AA. A novel optical sensor based on carbon dots embedded molecularly imprinted silica for selective acetamiprid detection. *Spectrochim Acta A Mol Biomol Spectrosc.* 2019;210:36–43.
 55. Watanabe E, Miyake S, Baba K, Eun H, Endo S. Immunoassay for acetamiprid detection: application to residue analysis and comparison with liquid chromatography. *Anal Bioanal Chem.* 2006;386:1441–8.
- Publisher's note** Springer Nature remains neutral with regard to jurisdictional claims in published maps and institutional affiliations.